Articles

Responsive Iron Neighboring Group Participation in Amino-Substituent-Stabilized [3]Ferrocenophane α-Carbenium Ions: A Combined Theoretical and Experimental Study

Patrick Liptau, Markus Neumann, Gerhard Erker,* Gerald Kehr, Roland Fröhlich,§ and Stefan Grimme*,#

Organisch-Chemisches Institut der Universität Münster, Corrensstrasse 40, D-48149 Münster, Germany

Received October 3, 2003

Treatment of the dimethylamino-[3]ferrocenophane **1a** with $B(C_6F_5)_3$ results in hydride abstraction at the $-CH(NMe_2)$ moiety in α-position to the ferrocene nucleus to yield the corresponding cation **4a**. The X-ray crystal structure analysis of the salt **4a**·$[HO\{B(C_6F_5)_3\}_2^-]$ has revealed a residual $Fe-C_\alpha$ interaction even in this case of a strongly substituent-stabilized α-ferrocenyl carbenium ion. A DFT calculation of a series of derivatives containing nitrogen substituents of a decreasing ability for carbenium ion stabilization (**4a**, $-NMe_2$; **4b**, −pyrrolyl; **4c**, −triazolyl) revealed a markedly increased Fe−C interaction with decreasing C^+ stabilization by the hetarene substituents.

Introduction

Ferrocene-based ligands have recently contributed significantly to the development of the use of selective homogeneous catalysts in organic synthesis and related areas. This holds for the open, nonbridged variants (e.g., of the "Josiphos" type)[1] but also increasingly for the bridged [*n*]ferrocenophane derivatives.[2,3] The stereoselective synthesis of most such ligands relies on the highly stereoselective conversion of ferrocene derivatives that bear reactive functional groups at the α-carbon atom of the metallocene substituent side chain. On the basis of early work by Ugi et al.[4] very effective anchimeric assistance of the central iron atom in the nucleophilic substitution of the α-substituents is well established to lead to overall retention of configuration via a double inversion pathway.[5,6] We have recently shown that the internal iron nucleophile is decisive even in the related S_N reactions in some chiral [3]ferrocenophane derivatives. We had presented evidence from a combined experimental and theoretical study[3] that the reactive intermediate **2** is formed in a first step starting from **1a** and is subsequently attacked from the outside by an external nucleophile (e.g., R_2P^-) to form **3** by overall retention of configuration. Variants of this very effective stereoselective reaction sequence have been used to prepare interesting new catalyst systems used in alternating CO/olefin copolymerization,[3] and such pathways were also recently applied for the synthesis of optically active [3]ferrocenophane systems.[7]

§ X-ray crystal structure analysis.
# DFT calculations.

(1) Togni, A., Hayashi, T., Eds. In *Ferrocenes: Homogeneous Catalysis, Organic Synthesis, Materials Science*; VCH: Weinheim, 1995. Togni, A., Haltermann, R. L., Eds. In *Metallocenes: Synthesis, Reactivity, Applications*; Wiley-VCH: Weinheim, 1998. Josiphos: Togni, A.; Breutel, C.; Schnyder, A.; Spindler, F.; Landert, H.; Tijani, A. *J. Am. Chem. Soc.* **1994**, *116*, 4062−4066.

(2) Mernyi, A.; Kratky, C.; Weissensteiner, W.; Widhalm, M. *J. Organomet. Chem.* **1996**, *508*, 209−218. Gómez-de la Torre, F.; Jalón, F. A.; López-Agenjo, A.; Manzano, B. R.; Rodríguez, A.; Sturm, T.; Weissensteiner, W.; Martínez-Ripoll, M. *Organometallics* **1998**, *17*, 4634−4644. Jalón, F. A.; López-Agenjo, A.; Manzano, B. R.; Moreno-Lara, M.; Rodríguez, A.; Sturm, T.; Weissensteiner, W. *J. Chem. Soc., Dalton Trans.* **1999**, 4031−4039. Sturm, T.; Weissensteiner, W.; Mereiter, K.; Kégl, T.; Jeges, G.; Petölz, G.; Kollár, L. *J. Organomet. Chem.* **2000**, *595*, 93−101. Weissenbach, M.; Sturm, T.; Kalchhauser, K.; Kratky, C.; Weissensteiner, W. *Monatsh. Chem.* **2002**, *133*, 991−1009.

(3) Liptau, P.; Seki, T.; Kehr, G.; Abele, A.; Fröhlich, R.; Erker, G.; Grimme, S. *Organometallics* **2003**, *22*, 2226−2232.

(4) (a) Marquarding, D.; Klusacek, H.; Gokel, G.; Hoffmann, P.; Ugi, I. *J. Am. Chem. Soc.* **1970**, *92*, 5389−5393. Gokel, G.; Marquarding, D.; Ugi, I. *J. Org. Chem.* **1972**, *37*, 3052−3058. Hayashi, T.; Mise, T.; Fukushima, M.; Kagotani, M.; Nagashima, N.; Hamada, Y.; Matsumoto, A.; Kawakami, S.; Konishi, M.; Yamamoto, K.; Kumada, M. *Bull. Chem. Soc. Jpn.* **1980**, *53*, 1138−1151. (b) Reviews: Watts, W. E. *J. Organomet. Chem. Library* **1979**, *7*, 399−459. Pearson, A. J. *Metallo-Organic Chemistry*; Wiley: New York, 1985; p 319−322. (c) Theoretical work: Gleiter, R.; Seeger, R. *Helv. Chim. Acta* **1971**, *54*, 1217−1220. Gleiter, R.; Seeger, R.; Binder, H.; Fluck, E.; Cais, M. *Angew. Chem.* **1972**, *84*, 1107−1109. *Angew. Chem., Int. Ed. Engl.* **1972**, *11*, 1028−1030. Gleiter, R.; Schimanke, H.; Silverio, S. J.; Büchner, M.; Huttner, G. *Organometallics* **1996**, *15*, 5635−5640. Volland, M. A. O.; Kudis, S.; Helmchen, G.; Hyla-Kryspin, I.; Rominger, F.; Gleiter, R. *Organometallics* **2001**, *20*, 227−230.

(5) Caynela, E. M.; Xiao, L.; Sturm, T.; Manzano, B. R.; Jalón, F. A.; Weissensteiner, W. *Tetrahedron: Asymmetry* **2000**, *11*, 861−869. Manzano, B. R.; Jalón, F. A.; Gómez-de la Torre, F.; López-Agenjo, A. M.; Rodríguez, A. M.; Mereiter, K.; Weissensteiner, W.; Sturm, T. *Organometallics* **2002**, *21*, 789−802. Sturm, T.; Weissensteiner, W.; Spindler, F.; Mereiter, K.; López-Agenjo, A. M.; Manzano, B. R.; Jalón, F. A. *Organometallics* **2000**, *21*, 1766−1774, and references therein.

(6) Tainturier, G.; Chhor y Sok, K.; Gautheron, B. *C. R. Acad. Sci. Paris C* **1973**, 1269−1270. Chhor y Sok, K.; Tainturier, G.; Gautheron, B. *Tetrahedron Lett.* **1974**, *25*, 2207−2208. Chhor y Sok, K.; Tainturier, G.; Gautheron, B. *J. Organomet. Chem.* **1977**, *132*, 173−189.

10.1021/om034214b CCC: $27.50
Publication on Web 12/02/2003

Scheme 1

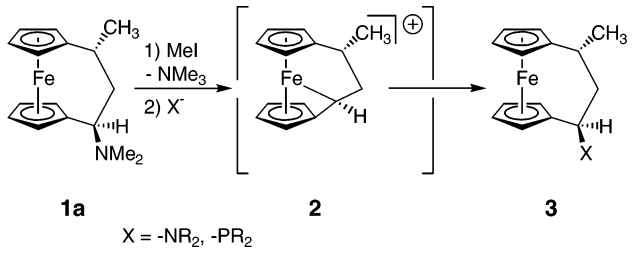

Scheme 2

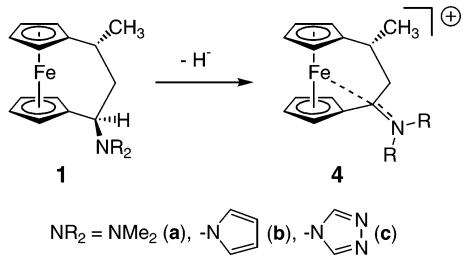

The intermediate **2** was characterized by DFT calculations.[3] The cationic system features a constrained framework structure, whose ligand geometry is quite different from that of its neutral precursor **1a**. In **2** the C_3-bridge is characterized by dihedral angles $\theta_1 = 42.9°$ (C1−C6−C7−C8) and $\theta_2 = -120.5°$ (C6−C7−C8−C11), which is very different from the usual "gauche-situation" found for the precursor **1a** ($\theta_1 = 65.6°$, $\theta_2 = -66.4°$).[3,7] The most striking structural feature of **2** is its strong α-C−Fe interaction (Fe−C8: 2.208 Å, calcd). This leads to a (η^6-fulvene)Fe-type structure[8] in which the exocyclic C11−C8 vector is bent from the mean C11 to C15 plane by $\beta = 42.8°$ *toward* the Fe atom (**1a**: $\beta = 4.1°$[3]). This posed the interesting question of the relative magnitude of the carbocation-stabilizing features of the iron metal center in such a coordinative environment relative to other competing cation-stabilizing groups such as an −OR or $-NR_2$ substituent. Achieving at least such a qualitative assessment is probably of general importance, but in addition of enormous practical significance for a further development of stereoselective ferrocene-type chelate ligand synthesis. We have, therefore, started to study such competition situations by DFT and experimental methods. First results, using a small series of $-NR_2$-substituted [3]ferrocenophane cation systems, have revealed a unique situation of an effective cationic delocalization between the stabilizing organic functional group and the participating central iron metal center. The iron center seems to be continuously "responding" to the competing electronic stabilization of the carbenium ion center in the [3]ferrocenophane bridge.

Results and Discussion

In the computational study we have formally removed a hydride from C8 of the complexes **1** to generate the cation systems **4** (see Scheme 2). The DFT-calculated structure of **4a** (NMe_2) shows the formation of a close to trigonally planar stabilized carbenium ion center at C8 (bond angles C7−C8−C11 119.1°, C7−C8−N 120.0°, C11−C8−N 120.8°). In the calculated structure **4a**(calcd) the carbenium ion is stabilized by a strong conjugative interaction with the adjacent nitrogen atom (C8−N: 1.325 Å), indicating the formation of an iminium ion-type compound. However, the DFT calculation has also revealed a pronounced "perpendicular" coordinative interaction of the C8 carbenium ion center with the iron atom. The calculated C8−Fe distance of 2.875 Å is markedly smaller than the geometrically imposed metal−α-carbon distance in the [3]ferrocene framework [calcd: 3.119 Å (Fe···C6)]. Consequently the [3]ferrocenophane framework in **4a**(calcd) is markedly distorted [θ_1 (C1−C6−C7−C8) = 60.7°, θ_2 (C6−C7−C8−C11) = −82.4°]. The C11−C8 vector in **4a**(calcd) is oriented considerably out of the adjacent C11 to C15 Cp-ligand plane *toward* the metal atom ($\beta_{calcd} = 13.7°$). This leads to a slight reduction of the Fe−C11 bond length (2.010 Å) relative to the Fe−(C12 to C15) (between 2.074 and 2.093 Å), Fe−C1 (2.038 Å), and Fe−(C2 to C5) bond lengths (between 2.055 and 2.075 Å, calcd).

An active competitive situation of stabilization of the sp^2-C8 carbenium ion center between the Fe atom and the adjacent nitrogen-containing substituent could respond sensitively to changes of the electron density of the nitrogen center. This can in principle be achieved by a formal exchange of the $-NMe_2$ substituent in **4a** for, for example, a *N*-pyrrolyl group, in which the lone pair at nitrogen is part of the aromatic π-system of the hetarene nucleus.[9]

The cation **4b**(calcd) was generated by formal H^- abstraction from C8 of the hypothetical *N*-pyrrolyl-substituted [3]ferrocenophane precursor system **1b**. As it may have been anticipated, the framework of the DFT-calculated structure **4b**(calcd) is substantially more distorted [θ_1 (C1−C6−C7−C8) = 52.6°, θ_2 (C6−C7−C8−C11) = −90.4°] as compared to **4a**(calcd). This is due to a much more pronounced coordinative interaction of the stabilized carbenium ion center C8 with the central iron atom. The Fe−C8 bond length amounts to 2.712 Å; that is, the iron−C8 bond in the −N-pyrrolyl-substituted system **4b**(calcd) is more than 0.16 Å *shorter* than the corresponding Fe−C8 interaction in the $-NMe_2$-stabilized complex **4a**(calcd). Consequently, the C11−C8 vector in **4b**(calcd) is even more strongly bent [$\beta = 21.7°$, which is almost halfway between the β-angle value of the neutral framework **1a** ($\beta = 4.1°$) and the parent cation **2**(calcd) ($\beta = 42.8°$)[3]]. The strong C11−C8 bending features are practically of no consequence in the found Fe−C(Cp) bond lengths in **4b**(calcd). (Fe−C11, 2.007 Å; Fe−(C12 to C15), 2.022−2.110 Å; Fe−C1, 2.047 Å; Fe−(C2 to C5), 2.059−2.079 Å). The coordination geometry of the carbon atom C8 in **4b**(calcd) has remained trigonal planar (angles C7−C8−C11, 121.9°; C7−C8−N, 118.1°; C11−C8−N, 119.9°), but the calculated C8−N bond length is slightly elongated at 1.357 Å. This

(7) Liptau, P.; Knüppel, S.; Kehr, G.; Kataeva, O.; Fröhlich, R.; Erker, G. *J. Organomet. Chem.* **2001**, *637*, 621−630. Liptau, P.; Tebben, L.; Kehr, G.; Wibbeling, B.; Fröhlich, R.; Erker, G. *Eur. J. Inorg. Chem.* **2003**, in press.

(8) Watanabe, M.; Motoyama, I.; Takayama, T. *J. Organomet. Chem.* **1996**, *524*, 9−18. Kupfer, V.; Thewalt, U.; Tišlerová, I.; Štěpnička, P.; Gyepes, R.; Kubišta, J.; Horáček, M.; Mach, K. *J. Organomet. Chem.* **2001**, *620*, 39−50. Harrington, L. E.; Vargas-Baca, I.; Reginato, N.; McGlinchey, M. J. *Organometallics* **2003**, *22*, 663−339, and references therein. See also: Williams, G. H.; Traficante, D. F.; Seyferth, D. *J. Organomet. Chem.* **1973**, *60*, C53−C56.

(9) This effect was recently used effectively in Lewis acid borane chemistry: Kehr, G.; Fröhlich, R.; Wibbeling, B.; Erker, G. *Chem. Eur. J.* **2000**, *6*, 258−266.

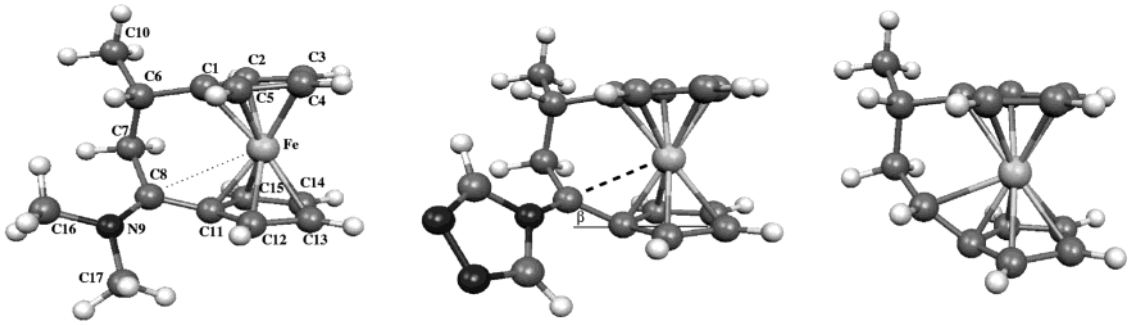

Figure 1. Views of the DFT-calculated structures of the cationic [3]ferrocenophane derivatives **4a**(calcd) (left) and **4c**(calcd) (center) and **2** (right). Selected bond lengths (Å) and angles (deg) of **4a**, (**4c**), and [**2**]: Fe−C8 2.875 (2.507) [2.208], Fe−C6 3.119 (3.101) [3.108], Fe−C1 2.038 (2.049) [2.075], Fe−(C2−C5) 2.055−2.075 (2.058−2.088) [2.075−2.090], Fe−C11 2.010 (1.990) [1.966], Fe−(C12−C15) 2.016−2.093 (2.037−2.135) [2.058−2.153], C1−C6 1.521 (1.525) [1.527], C6−C7 1.562 (1.561) [1.555], C7−C8 1.514 (1.518) [1.505], C8−C11 1.452 (1.426) [1.414], C8−N9 1.325 (1.384), C7−C8−N 120.0 (117.2), C11−C8−N 120.8 (118.6), β = 13.7 (30.5) [42.8].

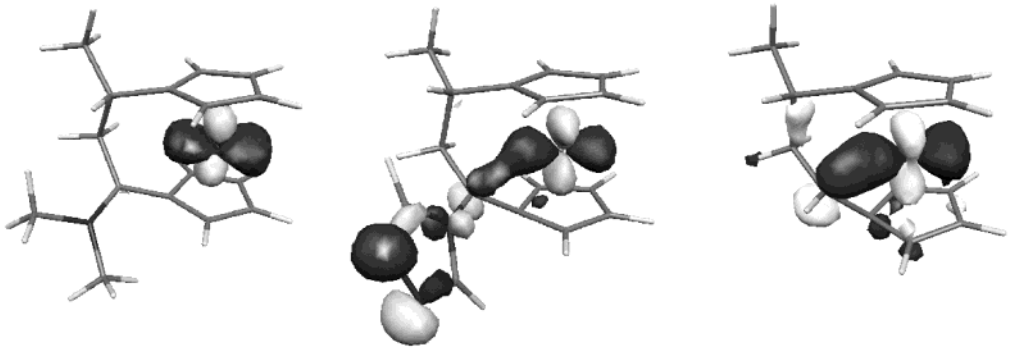

Figure 2. Isosurface plots (at a value of 0.05 $a_0^{(-3/2)}$) for the C8−Fe bonding MO of **4a** (left), **4c** (center), and **2** (right). The admixture of substituent amplitudes in the case of **4c** results from an accidentally close-lying substituent MO.

general trend is continued when the electron-withdrawing properties of the hetarene substituent are further increased. In the calculated structure of the *N*-triazolyl-substituted [3]ferrocenophane cation **4c**(calcd) (see Figure 1) the Fe−C8 interaction is even stronger (2.507 Å) and the bending of the C11−C8 vector from the adjacent Cp plane is even more pronounced (β = 30.5°).

The origin of the strong Fe−C8 interaction can already be understood in a simple orbital picture as provided for similar compounds by Gleiter et al.[4c] In Figure 2, the molecular orbital (MO) that is most responsible for the binding is displayed for the compounds already shown in Figure 1. In **4a** and **2** the bonding MO corresponds to HOMO−2 (i.e., HOMO and HOMO−1 are essentially nonbonding iron d orbitals), while it is HOMO−3 for **4c** due to an additional higher-lying MO of the substituent. The gradual increase of the Fe−C binding in the series **4a**, **4c**, and **2** is also reflected by an increasing stabilization of the corresponding orbital energy (−8.3, −9.9, and −10.4 eV for **4a**, **4c**, and **2**, respectively). The stronger interaction of the metal center with the carbon atom C8 is also clearly visible from the isosurface plots. The strongest overlap between the iron d_{xy} AO and the (formerly empty) carbon p AO occurs for **2** (R = H), it is significantly reduced for **4c**, and there are only negligible interactions for **4a** with the strong donor R = NMe_2.

We considered it desirable to have some of these remarkable calculated structural effects being supported by experimental evidence. For that purpose we chose

Scheme 3

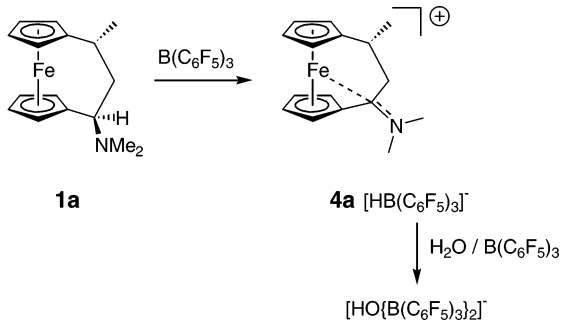

the system **4a**, where the supporting stabilization of the Fe center is probably most amazing and thus had to be most critically put to question. We thus prepared the complex **1a** starting from 1,1′-diacetylferrocene by means of a reaction sequence involving a Mannich-type coupling,[10,11] followed by catalytic hydrogenation, as it was previously described by us.[3,7] Hydride abstraction was then effected by treatment with the strong boron Lewis acid tris(pentafluorophenyl)borane.[12,13] The reaction of

(10) Knüppel, S.; Fröhlich, R.; Erker, G. *J. Organomet. Chem.* **1999**, *586*, 218−222; **2000**, *595*, 307−312.

(11) Knüppel, S.; Erker, G.; Fröhlich, R. *Angew. Chem.* **1999**, *111*, 2048−2051; *Angew. Chem., Int. Ed.* **1999**, *38*, 1923−1926. Bai, S. D.; Wei, X.-H.; Guo, J.-P.; Liu, D.-S.; Zhou, Z.-Y. *Angew. Chem.* **1999**, *111*, 2051−2054; *Angew. Chem., Int. Ed.* **1999**, *38*, 1926−1928.

(12) Massey, A. G.; Park, A. J.; Stone, F. G. A. *Proc. Chem. Soc. London* **1963**, 212. Massey, A. G.; Park, A. J. *J. Organomet. Chem.* **1964**, *2*, 245. Massey, A. G.; Park, A. J. *Organometallic Syntheses*; King, R. B., Eisch, J. J., Eds.; Elsevier: New York, 1986; Vol. 3, p 461.

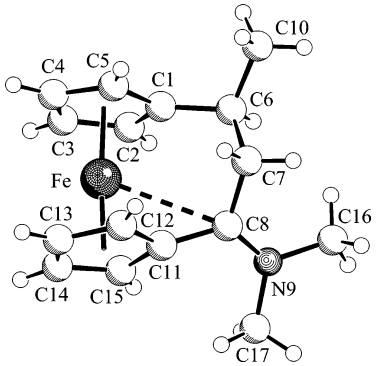

Figure 3. Molecular structure of the **4a**·[HO{B(C_6F_5)$_3$}$_2^-$] salt (only the cation is depicted). Selected bond lengths (Å) and angles (deg): Fe−CCp 1.998(2)−2.074(2), Fe−C6 3.111(2), Fe−C7 3.221(2), Fe−C8 2.873(2), C1−C6 1.512(3), C6−C7 1.548(3), C6−C10 1.536(3), C7−C8 1.508(3), C8−C11 1.454(3), C8−N9 1.300(3), N9−C16 1.482(3), N9−C17 1.475(3); C1−C6−C7 111.4(2), C1−C6−C10 111.7(2), C10−C6−C7 109.1(2), C6−C7−C8 111.9(2), C7−C8−N9 119.7(2), C7−C8−C11 118.9(2), C11−C8−N9 121.3(2), C8−N9−C16 122.9(2), C8−N9−C17 122.9(2), C16−N9−C17 114.2(2); C6−C7−C8−N9 92.9(2).

1a with B(C_6F_5)$_3$ took place smoothly and selectively at room temperature in CH_2Cl_2 solution. After ca. 30 min the reaction was complete, and the cationic product **4a** was isolated as a deep purple-colored product with [HB(C_6F_5)$_3^-$] anion: ^{11}B NMR δ (CD_2Cl_2, 25 °C) −25.5 (d, $^1J_{BH}$ = 91 Hz) in >70% yield.

The thus prepared complex **4a**·[HB(C_6F_5)$_3^-$] shows eight well-separated C_5H_4 ^{1}H NMR signals (values are given in the Experimental Section), a pair of −N(CH_3)$_2$ singlets, a doublet of the protons of the CHCH_3 substituent, in addition to the multiplets of the −CH−CH_2−C− [3]ferrocenophane bridge. The [HB(C_6F_5)$_3^-$] anion ^{1}H NMR resonance is found at δ 1.76 (in d_8-toluene). In addition, the ^{13}C NMR spectrum of **4a** shows the "iminium-ion" resonance (C8) at δ 193.1 (and two ipso-C Cp signals at δ 96.5 (C1) and 70.1 (C11)).

Crystallization at 4 °C over 7 days eventually gave single crystals suitable for X-ray crystal structure determination. It turned out that the original [HB(C_6F_5)$_3^-$] counteranion had selectively become hydrolytically changed into the [HO{B(C_6F_5)$_3$}$_2$]$^-$ monoanion (see Figure 4) during the crystallization process, but the cation had remained untouched. It shows almost the identical characteristic structural features that had already been revealed by the DFT calculation. In the crystal the cation **4a** shows a pronounced C8−Fe interaction at 2.873(2) Å (calcd: 2.875 Å), and the bending angle of the C11−C8 vector in **4a** amounts to 13.1° (calcd: 13.7°). This close agreement between calculated and experimentally derived features is found for most structural parameters of the cation **4a** (see Figures 1 and 3). This leads us to conclude that the iron atom in this family of [3]ferrocenophane-derived cations can adopt a stereochemically active role even in cases where a large competing electronic stabilization of the α-carbenium ion prevails, but the ensuing metal−C$^+$ interaction seems to very sensitively respond to changes in the electronic environment of the stabilized carbenium ion.

(13) Blaschke, U.; Erker, G.; Nissinen, M.; Wegelius, E.; Fröhlich, R. *Organometallics* **1999**, *18*, 1224−1234. Blaschke, U.; Menges, F.; Erker, G.; Fröhlich, R. *Eur. J. Inorg. Chem*. **1999**, 621−632.

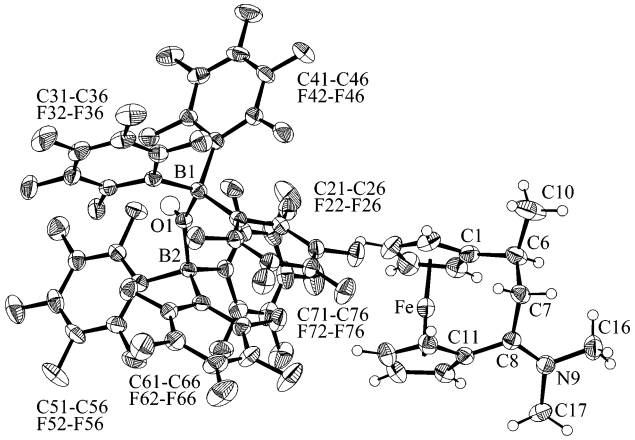

Figure 4. View of the molecular structure of the salt **4a**·[HO{B(C_6F_5)$_3$}$_2^-$]. Selected bond lengths (Å) and angles (deg) of the anion: O1−H1 0.78(2), O1−B1 1.572(3), O1−B2 1.565(3), B1−C21 1.631(3), B1−C31 1.647(3), B1−C41 1.656(3), B2−C51 1.655(3), B2−C61 1.635(3), B2−C71 1.649(3), C−C 1.363(3)−1.392(3), C−F 1.341(2)−1.359(2); B1−O1−H1 110(2), B2−O1−H1 108(2), B1−O1−B2 141.4(2), O1−B1−C21 107.0(2), O1−B1−C31 109.1(2), O1−B1−C41 106.8(2), O1−B2−C51 107.6(2), O1−B2−C61 106.6(2), O1−B2−C71 109.2(2), C21−B1−C31 115.1(2), C21−B1−C41 114.0(2), C31−B1−C41 104.5(2), C51−B2−C61 112.4(2), C51−B2−C71 104.8(2), C61−B2−C71 116.0(2).

Chemical consequences of this remarkably responsive organometallic neighboring group participation will be investigated in our laboratory.

Experimental Section

Technical Details of the Quantum Chemical Calculations. The calculations were performed with the TURBOMOLE suite of programs.[14a] All structures were fully optimized without any symmetry restrictions at the density functional (DFT) level employing the BP86 functional,[14b] a large Gaussian AO basis of valence-triple-ζ quality with two sets of polarization functions (TZV2P: C [5s3p2d], Fe [6s5p3d], H [3s2p])[14c,e] and the resolution-of-the-identity (RI) approximation to represent the Coulomb operator.[14d,e] Tests performed including f-functions on C, N, and Fe revealed minor changes (<0.002 Å for r_e, <0.5° for angles) of the calculated structural parameters. Further calculations of the Cartesian second derivatives were carried out yielding only real vibrational frequencies. The BP86 density functional was chosen because of its outstanding performance for the prediction of ferrocene structures (hybrid functionals such as the popular B3LYP usually yield too long Fe ring distances).

Technical Details of the X-ray Structure Analysis. X-ray crystal structure analysis of 4a: Formula $C_{16}H_{20}NFe$·HO{B(C_6F_5)$_3$}$_2$, M = 1323.17, red crystal 0.35 × 0.20 × 0.10 mm, a = 14.096(1) Å, b = 20.846(1) Å, c = 16.593(1) Å, β = 92.04(1)°, V = 4872.7(5) Å^3, ρ_{calc} = 1.804 g cm^{-3}, μ = 4.69 cm^{-1}, empirical absorption correction (0.853 ≤ T ≤ 0.955), Z = 4,

(14) (a) Ahlrichs, R.; Bär, M.; Baron, H.-P.; Bauernschmitt, R.; Böcker, S.; Ehrig, M.; Eichkorn, K.; Elliott, S.; Furche, F.; Haase, F.; Häser, M.; Horn, H.; Huber, C.; Huniar, U.; Kattannek, M.; Kölmel, C.; Kollwitz, M.; May, K.; Ochsenfeld, C.; Öhm, H.; Schäfer, A.; Schneider, U.; Treutler, O.; von Arnim, M.; Weigend, F.; Weis, P.; Weiss, H. *TURBOMOLE* (Vers. 5.5); Universität Karlsruhe, 2002. (b) Becke, A. D. *Phys. Rev. A* **1988**, *38*, 3098−3100. Perdew, J. P. *Phys. Rev. B* **1986**, *33*, 8822−8824. (c) Schäfer, A.; Horn, H.; Ahlrichs, R. *J. Chem. Phys.* **1992**, *97*, 2571−2577. (d) Eichkorn, K.; Treutler, O.; Öhm, H.; Häser, M.; Ahlrichs, R. *Chem. Phys. Lett.* **1995**, *240*, 283−289. (e) All basis sets are available from the TURBOMOLE homepage, http://www.turbomole.com, via FTP server button (in the subdirectories basen (AO basis sets) and jbasen (RI basis sets)).

monoclinic, space group $P21/n$ (No. 14), $\lambda = 0.71073$ Å, $T = 198$ K, ω and φ scans, 32 027 reflections collected ($\pm h$, $\pm k$, $\pm l$), [(sin θ)/λ] = 0.66 Å^{-1}, 11 568 independent ($R_{int} = 0.046$) and 7381 observed reflections [$I \geq 2\sigma(I)$], 791 refined parameters, $R = 0.043$, $wR_2 = 0.088$, max. residual electron density 0.26 (−0.43) e Å^{-3}, hydrogen at O from difference Fourier calculation, others calculated and all refined as riding atoms.

Data set was collected with Nonius KappaCCD diffractometer, equipped with a Nonius FR591 rotating anode generator. Programs used: data collection COLLECT (Nonius B.V., 1998), data reduction Denzo-SMN (Z. Otwinowski, W. Minor, *Methods Enzymol.* **1997**, *276*, 307−326), absorption correction SORTAV (R. H. Blessing, *Acta Crystallogr.* **1995**, *A51*, 33−37; R. H. Blessing, *J. Appl. Crystallogr.* **1997**, *30*, 421−426), structure solution SHELXS-97 (G. M. Sheldrick, *Acta Crystallogr.* **1990**, *A46*, 467−473), structure refinement SHELXL-97 (G. M. Sheldrick, Universität Göttingen, 1997), graphics SCHAKAL (E. Keller, Universität Freiburg, 1997) and DIAMOND (K. Brandenburg, Universität Bonn, 1997).

Crystallographic data (excluding structure factors) for the structure reported in this paper have been deposited with the Cambridge Crystallographic Data Centre as supplementary publication CCDC-211483. Copies of the data can be obtained free of charge on application to The Director, CCDC, 12 Union Road, Cambridge CB2 1EZ, UK [fax: int. code +44(1223)336-033, e-mail: deposit@ccdc.cam.ac.uk].

General Procedures. Reactions were carried out under an atmosphere of argon using standard Schlenk-type glassware or a glovebox. Solvents were dried and distilled under argon prior to use. Complex **1a** was prepared as previously described by us.[10] For additional general information including a list of spectrometers used for physical characterization see refs 3 and 7.

Reaction of 1a with $B(C_6F_5)_3$; Formation of 4a. Dichloromethane (40 mL) was added to a solid mixture of **1a** (1.00 g, 3.50 mmol) and $B(C_6F_5)_3$ (1.84 g, 3.60 mmol). The resulting solution was kept for 30 min at room temperature with stirring. Solvent was then removed in vacuo. The residue was suspended in pentane, and the solid product **4a**·[$HB(C_6F_5)_3^-$] was collected by filtration. Yield: 2.07 g (74%). Anal. Calcd for $C_{34}H_{21}BF_{15}FeN$ (795.2): C 51.36, H 2.66, N 1.76. Found: C 50.51, H 2.65, N 1.79. Cation: ^{1}H NMR (600 MHz, CD_2Cl_2, 298 K): δ 5.20, 4.85, 4.71, 4.64 (each m, each 1 H; 12-H to 15-H), 4.99, 4.78, 4.18, 4.01 (each m, each 1 H; 2-H to 5-H), 3.63 (m, 1 H; 7-H), 3.62, 3.59 (s, 3 H; 16/17-H), 3.36 (m, 1 H; 6-H), 2.91 (m, 1 H; 7-H), 1.38 (d, $^3J_{H,H} = 8.0$ Hz, 3 H; 10-H). ^{13}C{^{1}H} NMR (150 MHz, CD_2Cl_2, 298 K): δ 193.1 (C-8), 96.5 (C-1), 77.9, 76.4, 75.7, 68.5 (C-12 to C15), 73.6, 72.4, 70.4, 70.0 (C-2 to C-5), 70.1 (C-11), 49.2 (C-7), 48.0, 45.0 (C-16/17), 40.3 (C-6), 22.5 (C-10). Anion: ^{1}H NMR (600 MHz, C_7D_8, 298 K): δ 1.76. ^{13}C{^{1}H} NMR (150 MHz, CD_2Cl_2, 298 K): δ 150.0 ($^1J_{C,F} = 243$ Hz; *o*-Ph^F), 139.8 ($^1J_{C,F} = 243$ Hz; *p*-Ph^F), 138.4 ($^1J_{C,F} = 243$ Hz; *m*-Ph^F), 126.8 (br; *i*-Ph^F). ^{11}B NMR (64 MHz, CD_2Cl_2, 298 K): δ −25.5 (d, $^1J_{BH} = 91$ Hz). ^{19}F NMR (563 MHz, CD_2Cl_2, 298 K): δ −134.5 (m, 2 F; *m*-Ph^F), −164.7 (t, $^3J_{F,F} = 21$ Hz, 1 F; *p*-Ph^F), −167.8 (m, 2 F; *o*-Ph^F).

Acknowledgment. Financial support from the Fonds der Chemischen Industrie and the Deutsche Forschungsgemeinschaft is gratefully acknowledged.

Supporting Information Available: Detailed information about the X-ray crystal structure analyses of **4a**·[$HO\{B(C_6F_5)_3\}_2^-$]. This material is available free of charge via the Internet at http://pubs.acs.org.

OM034214B